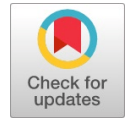


An Overview of Deep Learning Methods for Segmenting Thyroid Ultrasound Images

Jatinder Kumar, Surya Narayan Panda, Devi Dayal



Abstract: One of the various imaging modalities that is most frequently utilized in clinical practice is ultrasound (US). It is an emerging technology that has certain advantages along with disadvantages such as poor imaging quality and a lot of fluctuation. To aid in US diagnosis and/or to increase the objectivity and accuracy of such evaluation, effective automatic US image assessment techniques must be created from the perspective of image analysis. The most effective machine learning technology, notably in computer vision and general evaluation of images, has since been proven to belong to deep learning. Deep learning also has a huge potential for using US images for many automated activities. This paper quickly presents many well-known deep learning architectures before summarizing and delving into their applications in a number of distinct.

Keywords: Deep learning, Ultrasound Image, Segmentation, Thyroid Nodule, Deep Learning, Machine Learning

I. INTRODUCTION

A branch of computer science that makes an effort to make PCs smarter is Artificial Intelligence (AI). Incorporating intelligence into an aspect of interest is one of the necessary necessities for any intelligent actions. A large part of scholars these days accept that without learning intelligence, there is no intelligence. Since the very beginning, ML structures have been used to test scientific information units. Recognition of ML and statistical patterns is the most important discipline in biomedical society because they advocate assurance to increase the sensitivity and precision of discovery and diagnosis of an ailment, even though the objectivity of choice making mechanism is defined. In clinical science, diagnosis is a big challenge since it is important in deciding whether or not a patient has the disease which assists to define the effective course of treatment for the diagnosed disorder. A hot research field of computer science has been the application of techniques for disease diagnosis using intelligent algorithms [1].

II. DEEP LEARNING

Deep learning which is subdivision of ML that includes computing hierarchical features or depictions of sample facts (for example, photographs) by combining lower level abstract qualities, higher level abstract qualities are formed [2]. DLC can process raw images straight, eliminating the necessity of preprocessing, dissection, and feature abstraction. Major DL methods necessitate image scaling due to the input value constraint. Some processes call for force normalization and contrast enhancement that may be evaded by employing the facts augmentation methods deliberated late in the passage. As a result, DLC improves classification accuracy by avoiding issues like erroneous feature vectors and sloppy segmentation. The feature vector is fed into a machine learning classifier, which produces the object class, whereas the picture is fed into a deep learning classifier, which produces the object class. It's worth noting that deep learning is theoretically superior to regular artificial neural networks (ANN) because this one has additional layers [3]. Representable learning occurs when each layer translates the preceding layer's response facts into a new depiction at advanced and additional abstract level. That all level of a deep learning network, a nonlinear purpose transforms data into representation. In most circumstances, the occurrence or nonappearance of edges in precise arrangements, as well as their location in the image, can be determined using attributes gained from an image's initial layer of representation. The second layer detects edge location while ignoring slight changes, and the third layer combines these patterns into higher groupings that match to sections of comparable matters, allowing subsequent layers to recognise objects using these groupings [4]. Deep learning's remaining efficiency for variety of artificial intelligence uses is due to this hierarchical feature representation, which learns straight via response. Figure 1 shows how ML and DLC techniques relate to one another [5].

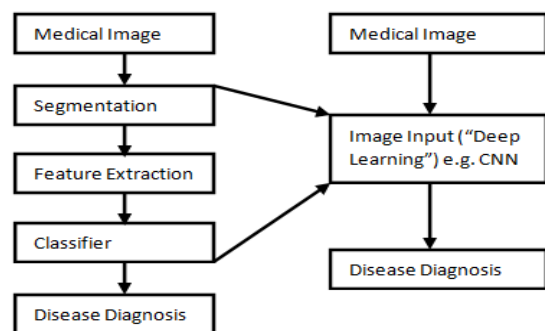


Fig. 1. Machine Learning and Deep Learning

Manuscript received on 04 November 2023 | Revised Manuscript received on 12 December 2023 | Manuscript Accepted on 15 December 2023 | Manuscript published on 30 December 2023.

*Correspondence Author(s)

Jatinder Kumar*, Institute of Engineering and Technology, Chitkara University, Punjab, India. Email: kumar.jatinder@pgimer.edu.in

Surya Narayan Panda, Institute of Engineering and Technology, Chitkara University, Punjab, India. E-mail: snpanda@chitkara.edu.in

Devi Dayal, Department of Paediatrics, Endocrinology and Diabetes Unit, PGIMER, Chandigarh, India. drdevidayal@gmail.com

© The Authors. Published by Blue Eyes Intelligence Engineering and Sciences Publication (BEIESP). This is an open access article under the CC-BY-NC-ND license <http://creativecommons.org/licenses/by-nc-nd/4.0/>

III. ARCHITECTURE OF DEEP LEARNING

A. Convolutional Neural Network (CNN)

Because it is like to standard NN, CNN is the most often used deep learning architecture. Contrasting a traditional NN (displayed in Figure 2a), CNN responds to a picture and has a triple dimensional structure of neurons to only connect to a little fraction of the prior level rather than the whole level (displayed in Figure 2b). The convolutional layer makes bulks of feature maps comprising the filter's retrieved features by performing a convolution operation among pixels in the response picture and a strainer. The nonlinear activation layer of ReLU which increases nonlinearity and training speed by applying the function $f(x) = \max(0, x)$ on reply inputs [6]. CNN is frequently used to tackle classification problems, as previously indicated. To practice CNN for semantic dissection, response picture was distributed among minor squares of the identical magnitude. Patch is then progressive to the next pixel in the center to be classified. However, because the corresponding topographies of the sliding squares are not reprocessed, the image loses spatial information of topographies travel to finishing completely interconnected layers of network which approach is inefficient. To resolve this difficulty, the FCN was suggested (shown in Figure 2).

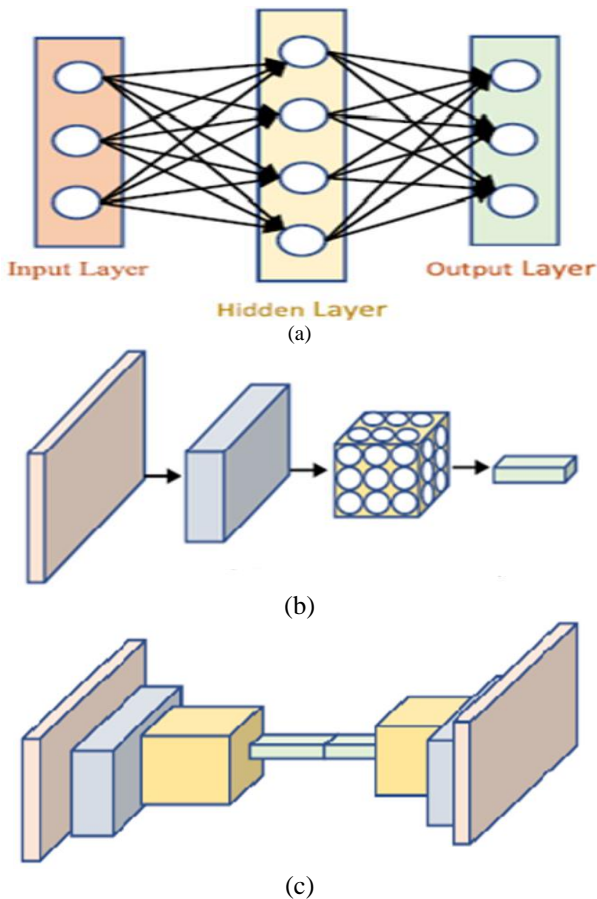


Fig. 2. Types of Neural Network (A) Traditional Neural Network (B) Convolutional Neural Network (C) Fully Convolutional Neural Network

B. Restricted Boltzmann Machines (RBMs)

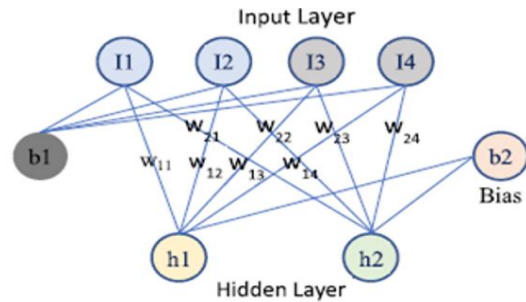


Fig. 3. Restricted Boltzmann Machines (RBMs)

The dominance of the accessible energy functions is determined using the loss function that is minimised during learning. Established with plan displayed in figure 3, the RBM's energy function with ai weighted inputs can be written as:

$$E(I, h) = - \sum_i a_i I_i - \sum_j b_j h_j - \sum_{i,j} I_i h_j w_{i,j} \quad (1)$$

C. Autoencoder based Deep Learning architectures

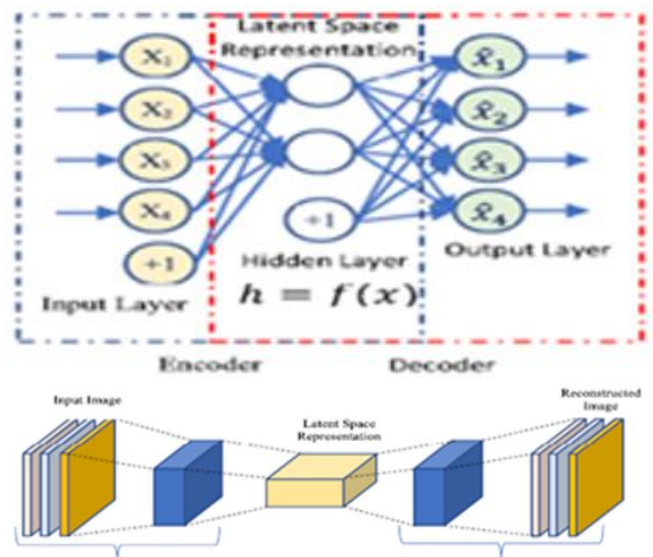


Fig. 4. Autoencoder Architectures with Vector

Autoencoders have insufficient applicability and are not appropriate as generative models because of breaks in latent space descriptions. It was decided to develop variational autoencoders to deal with this issue. For a variational autoencoder, the encoder produces two encoded vectors rather than a single encoded vector. The means vector is one, and the standard deviations vector is the other. These vectors are used as inputs to an accidental adjustable that samples productivity encoded vector. Figure 4 depicts the design of an Autoencoder.

D. Sparse Coding based Deep Learning Architectures

Unsupervised learning that uses a disproportionately large number of basis vectors to represent the input data is referred to as sparse coding. When the measurement of the latent portrayal is more than the input, the term "overcomplete" is employed.

The goal is to identify a linear mixture for these basis vectors that correlates to a certain response. Additional sparsity constraints must be implemented because the network is over finished in order to handle any degeneracy. Sparse coding has two advantages: finding linkages between related descriptors and capturing significant visual components.

E. Generative Adversarial Networks (GANs)

In order to develop a generator that, after training, tracks the desired distribution and accepts unplanned variables as response, GANs emulate a transform function using a neural network. A discriminator network is simultaneously taught to discriminate between false and real facts. The final grouping error between the created and actual data is the point at which the two networks compete against one another, each attempting to minimize or maximize it. As a result, each repeat of the training process improves both networks.

F. Recurrent Neural Networks (RNNs)

When the scale of the response is not anticipated, RNNs are designed to function with response types in sequence. Given that the input for the series has an effect on values nearby, the network must comprehend how it relates to the other inputs. RNNs are networks that produce current output based on both the input at hand and information learned from previous outcomes. The network stores the preceding response data in a hidden state vector. This means that depending on the inputs that came before it in the series, a single input could produce a wide range of outputs. The network generates distinct fixed-size output vectors when the input series values are changed frequently. Every input updates the concealed state. More hidden state layers, non-linear hidden layers between the response and the unknown state layer, additional layers between the unknown state layer and the output layer, or a mix of all three can be used to make RNNs deeper.

IV. DEEP LEARNING ARCHITECTURE IMPLEMENTATION METHODOLOGIES

(i) Picture segmentation procedures based on DL have been functional now a variety of methods. Because the neural network must be built and trained from start in the first technique, it is time-consuming and requires access to a big labelled dataset. The other strategy, some pre-trained CNNs, such as AlexNet, can be used to classify 1.2 million great tenacity photos for 1000 different classes [7]. This approach involves routinely removing the network's top tiers and replacing them with new, mission-specific layers. In early layers, low-level features learnt from millions of images are mixed with task-specific information acquired in the end layers to create a network for categorising fresh photos. They have the advantage of saving time when working because only a few weights need to be established. When trained on ImageNet data, transfer learning is more efficient than random weight initialization. The third method comprises extracting features from data using pre-trained CNNs and then utilising those features as inputs to train a traditional classifier like a support vector machine. This approach has the benefit of eliminating the need for time-consuming human feature abstraction by automatically extracting

features for a large number of category facts. U-Net and CNN are two well-known convolutional neural networks, which were recognised for volumetric medical image segmentation and V-Net, which was developed for biomedical picture subdivision. An FCN with two paths—one for contraction and the other for expansion—is referred to as a U-Net. A max-pooling layer and subsequent convolutional layers make up the contraction path [8-10].

A. Biomedical Images Types

Depending on the imaging technology, there are many sorts of biomedical images. Some of the most often utilised biomedical imaging methods are listed below.

B. Clinical Photographs

Clinical pictures are computerized pictures of a patient's body use to manuscript wounds, blisters, and skin limitations. These photos could be automatically analysed to monitor therapy efficacy completed period. Clinical photos are commonly recycled in dermatological and aesthetic dealings to pathway earlier and later skin or structural representations. Melanoma, a type of skin cancer, is most typically diagnosed via clinical pictures.

C. X-ray Imaging

When the result is a two-dimensional image, X-ray imaging is among the most commonly utilized imaging technique to detect fractures and bone dislocations. The National Institutes of Health (NIH) has released 100,000 chest x-ray images, along with relevant information and diagnoses, in order to develop imaging analysis tools [11]. The Massachusetts Institute of Technology (MIT) has similarly made a dataset of over 350,000 chest x-rays available for developing machine learning prototypes to recognize 14 frequent illnesses like pneumonia and punctured lung [12].

D. Computed Tomography (CT)

The CT, a computed imaging technique, uses 360-degree x-rays to create a comprehensive cross-sectional description of the inner body parts, bones, soft tissue, and blood basins of the body. The slanting plane, which is perpendicular to the body's long axis, is where most photographs are taken. These images can be triple dimensionalized by reformatting slices of them into several planes and combining them. Because CT solves biological imaging problems, it is frequently used to detect the presence and size of tumours and hence identify cancer.

E. Ultrasound Imaging (US)

Following the continued emergence of improved ultrasonic technology and the well-established US-based digital health system, US, a versatile green imaging modality, is developing globally as a first-line imaging approach in a variety of clinical sectors. High-frequency linear transducers (7.5-15.0 MHz) are used in the US, which may penetrate to a depth of up to 5 cm and generate high-definition images.

An Overview of Deep Learning Methods for Segmenting Thyroid Ultrasound Images

US is one of the most widely utilised imaging modalities and is regarded by practitioners and radiologist as a powerful tool for screening and diagnosis. The world over, US imaging has become popular in prenatal screening due to its virtual protection, low cost, noninvasive nature, real-time display, operator comfort, and experience. Several important advantages of US over additional medicinal scanning modalities like X-ray, magnetic resonance imaging (MRI) and CT have been established throughout the decades, including non-ionizing radiation, mobility, approachability, and price effectiveness [13]. As a result, various Thyroid Imaging Reporting and Data Systems based on US images have been built in recent years [14 – 17].

F. Magnetic Resonance Imaging (MRI)

In MRI imaging method a high magnetic fields use to create pictures of physiological progressions, organs, and tissues within the body. Non-bony bodily parts, also known as soft tissues, are imaged using MRI. CT scans and MRI are fundamentally different in that MRI uses ionizing radiation. In comparison to x-rays and CT scans, MRI scans provide better resolution for knee and shoulder problems. Neuroimaging datasets with roughly 2000 MRI sessions have been generated by the Open Access Series of Imaging Studies (OASIS) programme for biomedical scanning researchers [18].

G. Optical Coherence Tomography (OCT)

A low-coherence light is used in OCT technology to obtain micrometer-resolution, double-dimensional, and triple-dimensional images from within biological tissue. OCT is frequently used to identify eye issues because it provides a cross-sectional image of the retina that enables the practitioner to see each layer clearly. Now available are layer mapping and wideness evaluation, which were used for the conclusion.

H. Microscopic Images & Scintigraphy

Medical images taken at a microscopic level are utilised to assess the tissue's small structure. Biopsy is utilised to retrieve tissue for investigation, and subsequently staining components are employed to expose cellular features in areas of the tissue. Counter stains are used to give the graphics more colour, visibility, and contrast. This type of imaging is commonly used to diagnose malignancy. On a steady basis, the nucleus plus allocation of cells in the tissue, as well as their form and size, are all tested. Scintigraphy, often known as a thyroid scan, is performed in nuclear medicine. Scintigraphy is used to determine the active (functioning) portion of the thyroid gland. The patient is given a radioiodine drug, and then gamma cameras are used to capture photographs of the thyroid and reveal the part of the thyroid that uptakes iodine, i.e. the active or functional component of the thyroid. Scintigraphy imaging is a type of 2-D imaging that is used to examine the thyroid's function.

V. DATA AUGMENTATION

The enactment of DL neural networks was determined by handiness of appropriate facts. Facts augmentation, that includes removing a set of reasonable alterations to the samples (e.g., flip, rotate, mirror) in addition augmenting color (grey) values, is the greatest commonly use method for aggregate the extent of the training dataset. The efficiency of

data augmentation is examined in a non-clinical research, and the outcomes tell that classic augmentation methods can enrich by up to 7% [19-21] [37]. Various data augmentation strategies are used in the lack of real data to produce additional training data from the prevailing data pool. Augmentation strategies update figures in a way that preserves the class, and they can include things like: 1) Image translation: in this practice of moving image pixels in single track, either horizontally or vertically, without altering pictures overall dimension; 2) Image flipping: Flipping the image pixels horizontally and vertically by retreating the rows and columns of pixels; 3) Picture Rotation: Rotation of an picture from 0 to 360 degrees; 4) Contrast adjusting: Changing picture illumination levels to train the procedure to accommodate for such distinctions in test shots; 5) Image Zooming: Randomly increase in or out of the picture by adding fresh boundary pixels or using interpolation. Using nearest-neighbor fill, boundary pixel duplication, averaging, or interpolation, few existing pixels being deleted and fresh pixels being included in most of these techniques. The first four solutions are referred to as inflexible data augmentation strategies since the data shape remains unaltered. The fifth method keeps the vertical and horizontal augmentation ratios the same. If it's not the same, the picture will spread further in single way than the other (image stretching). Goal of these augmentation techniques is to make deep neural networks more generalizable while avoiding feature under-fitting and over-fitting. These strategies are usually applied mechanically throughout the network's training phase. Additional resolution is to transfer knowledge from successful models that have been implemented in the same (or even other) industries. In transfer learning the system trained to recognize and apply understanding educated in a prior origin domain to a fresh assignment. Transfer learning, on the other hand, is influenced by network structure, organ imaging modality, and dataset size [22] [38].

VI. QUANTITATIVE ANALYSIS

The objective analysis is a crucial metric for determining whether or not a segmentation algorithm is effective. The effectiveness of the picture segmentation system is evaluated using well-known benchmarks, enabling a comparison of the system to recently published methods in the literature. The choice of a suitable assessment metric is influenced by a number of variables, including the way the system is run. These metrics can be used to assess, among other things, the correctness, handling time, memory utilisation, and computational difficulty [23]. Table 2 defines the several abbreviations (TP, FP, FN, and TN) applied to evaluate the segmentation performance of deep learning prototypes:

TABLE 1: Abbreviations Applied to Evaluate the Segmentation Performance

Category	Actual Disease	Actual No Disease
Predicted Disease	True Positive (TP)	False positive (FP)
Predicted No Disease	False Negative (FN)	True Negative (TN)

(1) Accuracy

The most basic performance indicator is this one. An alternative term for it is overall pixel precision. The precision is in identifying whether a patient is unwell or healthy.

$$Accuracy = \frac{Correctly\ Predicted\ Pixels}{Total\ No.of\ Image\ Pixels} = \frac{TP+TN}{TP+FP+FN+TN} \quad (2)$$

(2) Precision/Specificity

Precision is the percentage of disease pixels in the programmed subdivision result that match the actual illness pixels. Precision serves as a useful benchmark of segmentation performance because it is susceptible to over-segmentation. The capability to precisely quantify healthy cases is referred to as specificity [24 – 26].

$$Precision = \frac{Correctly\ Predicted\ Disease\ Pixels}{Total\ No.of\ Predicted\ Disease\ Pixels} = \frac{TP}{TP+FP} \quad (3)$$

(3) DICE Similarity Coefficient (DSC)

DSC is superior to total pixel accuracy because it reflects equally false alarms and missed data in each class. DICE be too thought toward be real superior since it measures not just the amount of pixels that have been suitably identified, but also the precision with which the segmentation borders have been drawn [27]. Here S stands for segmentations in this case.

$$DICE = \frac{2 \times TP}{2 \times TP + FP + FN} \quad (4)$$

(4) Sensitivity / Recall

Sensitivity refers to the ability to accurately measure disease cases. The fraction of illness pixels in the ground truth which are exactly predicted using programmed segmentation is referred to as sensitivity.

$$Sensitivity = \frac{TP}{TP+FN} \quad (5)$$

(5) Jaccard Similarity Index

The percentage of the space of intersection among the anticipated subdivision and the ground fact subdivision to the region of merger among anticipated subdivision and the ground truth subdivision be called JSI (Intersection-Over-Union).

$$JSI = \frac{TP}{TP+FP+FN} \quad (6)$$

As can be seen from the above, there is a distinction between JSI and DSC.

$$JSI = \frac{DSC}{2-DSC} \quad DSC = \frac{2JSI}{1+JSI} \quad (7)$$

(6) Negative Predictive Value (NPV)

The likelihood that a disease does not exist given a negative test result is defined as [28]:

$$NPV = \frac{TN}{TN+FN} \quad (8)$$

VII. LITERATURE REVIEW

A review of various segmentation approaches for thyroid diagnosis using US images done. We looked at research that used deep learning prototypes aimed at biological picture separation. The table contains the editorial orientation, the modality, which describes the picturing methods applied for picture arrangement otherwise acquirement, the style, which describes the deep learning design use for subdivision, the comments part, which in brief describes the planned method, and lastly the performance metrics with brief descriptions

used to calculate the planned algorithm. The popular approaches, as are established on CNN or FCN. None of these articles engage in transfer learning, however one of them uses a DL model to extract features before using a structured support vector machine to classify the data. The most often used imaging modalities in these applications were US, CT, and MR, which reflects the direction of current research. The ease with which image datasets can be gathered through numerous competitions or other publicly available sources is one explanation for this.

Xu et al [29]. the suggested method divides US images of the breast into four major tissues: skin, fibro glandular tissue, mass, and fatty tissue using three orthogonal image planes. The addressed pixel's tissue class inside the image chunk is indicated by CNN. The quantitative criteria for evaluating segmentation outcomes, Accuracy, Precision, Recall, and F1 measure, all above 80%, indicating that the suggested technique is effective for differentiating practical tissues in breast US pictures. The recommended approach, according to the scientists, may provide the segmentations required to aid in the clinical breast cancer detection and enhance imaging in other US medical modes.

Badea et al [30]. to classify blaze photographs, researchers employed the LeNet CNN and Network in Network (NiN) designs. LeNet CNN was initially created in 1998 for the purpose of detecting handwritten numbers on currency. The burn picture database had 611 photographs of 53 paediatric patients through a resolution of 1664 × 1248 pixels. Clinical pictures are carefully crop to a dimension of 230 × 240 pixels. Outcome specified modest plan executed fine for binary classification difficulties, but that as the problems became more complicated, performance dropped substantially.

Kaur et al [31]. the ACEW, DRLSE, and LRBAC (Localized Region Based Active Contour) subdivision methods were described. The forefront and backdrop are discussed for minor regions using this strategy. Every point is considered separately in order to optimise the local energy. Every spot was analysed independently near optimise confined power in order to minimise the power compute in its own limited area. Physical initialization of the mask is required, as is manual parameter change. The distance regularisation term and the external energy term are used in DRLSE to drive the contour to the desired edges.

Poudel et al [32]. concluded that ML techniques generate more accurate and efficient segmentation, but they necessitate a large number of tagged datasets and longer training time. According to the authors, 3D U-Net CNN exists an mechanical subdivision technique for 3-D US pictures that uses a decoder to provide full-resolution subdivision and an encoder to analyse whole image by contracting in every succeeding layer. Although it does take additional training time, this technique has the advantage of being able to partition 3D thyroid glands without the usage of handcrafted characteristics. The CNN prototype has greatest average dice coefficient (DC) of all the segmentation outcomes, at 87.6%.

An Overview of Deep Learning Methods for Segmenting Thyroid Ultrasound Images

Random forest (RF) and decision tree (DT), which are non-automated segmentation methods, are two other approaches. This approach has a low computing complexity but is sensitive to certain characteristics. The results of the DC, RF, and DT techniques are 86.20 %, 67.00 %, and 86.20 %, correspondingly.

Shenoy et al [33]. have proposed Improved U-Net for the probable identification of ROI by segmentation. To achieve greater efficiency, two feature maps, high level and low level, have been explored. The use of these two feature maps helps to avoid low resolution. Further, the Improved U-Net is tested using the standard dataset DDTI in three sections. First, ROI is compared, which demonstrates that existing models have different ROI than ground models because to limited resolution, but our model has a better ROI. The authors compare the model's True Positive Rate and Dice Coefficient, achieving 98.95 and 95.60, respectively. Furthermore, the model outperforms the previous model by 2.51% and 3.36 %, respectively, according to the comparison analysis. Finally, the author found that, while the Improved U-Net obtains substantial performance when compared to the present model of segmentation, it can still be improved when batch normalization is taken into account.

Garg et al [34]. created a method for generating a classifier that was trained using a supervised learning algorithm; however, the method was only evaluated on a dataset of five photos. In this study, a feed forward neural network was built to segment the thyroid gland region. Image enhancement, feature extraction, Functional Neural Network (FNN) training and arrangement are among the procedures. This technique uses texture as a criterion in image segmentation. Sensitivity and Specificity, which are 89.06 % and 98.90 %, respectively, are used to assess performance.

Frannita et al [35] [39]. analysed US photos to identify thyroid cancer into three categories based on internal content characteristics. The nodular feature can be used to diagnose thyroid cancer. The time it takes a radiologist to diagnose a thyroid nodule is determined by their experience. Automated method is required to eradicate radiologist dependence. This research focuses on exploiting textural cues to categorise thyroid nodules into three groups. A total of 97 thyroid US pictures were used in this study. The suggested method's initial step is pre-processing, which is utilised to improve detection capability. Then, to find the correct nodules, morphological operation and active contour are used. Histogram, GLCM, GLRLM, and lacunarity are used to extract the segmented area. Multilayer Perceptron (MLP) is used to classify the data based on the extracted value. The achieved precision of 98.97 %, kindness of 98.92 %, specificity of 99.47 %, PPV of 99.05 %, and NPV of 99.50 %. Lacunarity feature was found to be effective in classifying three classes.

Ying et al. [36] researchers observed that using thyroid nodule segmentation in the form of cascaded thyroid nodule convolution, they were able to locate an exact position for nodules in thyroid ultrasound images, as well as its aspect ratio, margin, and figure. They came to the decision that the aspect ratio and margin form of nodules in thyroid US pictures affect the doctor's opinion. The proposed method not only aids doctors in locating individual nodules, but it also offers indicative information like margin, shape, and aspect

ratio of the nodule. The segmentation outcomes of nodules with sophisticated margin details are not precise enough in the experimental findings, indicating that FCN still has some shortcomings in terms of accurate segmentation and that it is tough to reestablish all details by up-sampling and interpolation.

VIII. CONCLUSIONS

In this study of deep learning systems for US image segmentation, certain key concerns were addressed. All of these research used real-world data to show that the proposed technique worked in specific applications with small datasets. The question of why deep learning algorithms work for a specific problem is still open. The solution to this problem is currently a work in progress. Network performance will suffer as a result of the lack of generalizability. The demand for incredibly large image databases is another challenge with DLC networks. As a result, a lot of storage and memory will be required, as well as a large amount of training time for the networks. Another important research area is the decrease of training time as well as the proper management of massive volumes of imaging data in terms of storage and memory requirements. DLC centered methods for biological requests in clinical practice have also been hampered by a lack of large enough imaging datasets. As a result, efforts must be made to make such data agreeably accessible, whether over outstanding test struggles or facts offerings, because the longstanding paybacks of facts distribution outlying compensate every small time achievements obtained by keeping facts secreted. If more captioned photographs are made publically available, more can be done. Manual labelling of visual figures by experts continues to be a substantial hurdle to ground truth generation. In the absence of ground information, unsupervised learning methodologies should receive more consideration.

DECLARATION STATEMENT

Funding	No, did not receive fund from any resources.
Conflicts of Interest	No conflicts of interest to the best of our knowledge.
Ethical Approval and Consent to Participate	No, the article does not require ethical approval and consent to participate with evidence.
Availability of Data and Material	In this research work authors used publicly available data across Ecommerce websites.
Authors Contributions	All authors having equal participation in the article.

REFERENCES

1. Vemulapalli L, SekharPC., Indian Journal of Applied Research, 9, p. 398 (2019).
2. Deng, L. and Yu, D., Foundations and trends in signal processing, 7(3-4), p.197 (2014). <https://doi.org/10.1561/20000000039>
3. Shen, D., Wu, G. and Suk, H.I., Annual review of biomedical engineering, 19, p.221 (2017). <https://doi.org/10.1146/annurev-bioeng-071516-044442>

4. Wang, G., IEEE, 4, p.8914 (2016). <https://doi.org/10.1109/ACCESS.2016.2624938>
5. Suzuki, K., Radiological physics and technology, 10(3), pp.257 (2017). <https://doi.org/10.1007/s12194-017-0406-5>
6. Vemulapalli L, SekharPC., Indian Journal of Applied Research, 9, p. 398 (2019).
7. Krizhevsky, A., Sutskever, I. and Hinton, G.E., Advances in neural information processing systems, 25, p.1097 (2012).
8. Garcia-Garcia, A., Orts-Escolano, S., Oprea, S., Villena-Martinez, V., Martinez-Gonzalez, P. and Garcia-Rodriguez, J., Applied Soft Computing, 70, p.41 (2018). <https://doi.org/10.1016/j.asoc.2018.05.018>
9. Ronneberger, O., Fischer, P. and Brox, T., International Conference on Medical image computing and computer-assisted intervention p. 234 (2015). https://doi.org/10.1007/978-3-319-24574-4_28
10. Milletari, F., Navab, N. and Ahmadi, S.A., Fourth international conference on 3D vision (3DV), p.565 (2016).
11. N. I. of H.-C. Center. Chest X-ray NIHCC. [Online]. Available, <https://nihcc.app.box.com/v/ChestXray-NIHCC> [Accessed: 10-Nov-2021] (2017).
12. T. M. I. of T. (MIT)'s L. for C. Physiology. MIMIC-chest X-ray database (MIMIC-CXR) [Online]. Available, <https://physionet.org/content/mimic-cxr/2.0.0/> [Accessed: 10-Nov-2021].
13. Reddy, U.M., Filly, R.A. and Copel, J.A., Obstetrics and gynecology, 112(1), p.145 (2008). <https://doi.org/10.1097/01.AOG.0000318871.95090.d9>
14. Haugen, B.R., Alexander, E.K., Bible, K.C., Doherty, G.M., Mandel, S.J., Nikiforov, Y.E., Pacini, F., Randolph, G.W., Sawka, A.M., Schlumberger, M. and Schuff, K.G., The American Thyroid Association guidelines task force on thyroid nodules and differentiated thyroid cancer, 26(1), pp.1(2016). <https://doi.org/10.1089/thy.2015.0020>
15. Gharib, H., Papini, E., Paschke, R., Duick, D.S., Valcavi, R., Hegedüs, L. and Vitti, P., Journal of endocrinological investigation, 33(5), p.287 (2010). <https://doi.org/10.1007/BF03346587>
16. Kwak, J.Y., Han, K.H., Yoon, J.H., Moon, H.J., Son, E.J., Park, S.H., Jung, H.K., Choi, J.S., Kim, B.M. and Kim, E.K., A step in establishing better stratification of cancer risk. Radiology, 260(3), p. 892 (2011). <https://doi.org/10.1148/radiol.11110206>
17. Park, J.Y., Lee, H.J., Jang, H.W., Kim, H.K., Yi, J.H., Lee, W. and Kim, S.H., A proposal for a thyroid imaging reporting and data system for ultrasound features of thyroid carcinoma. Thyroid, 19(11), p.1257 (2009). <https://doi.org/10.1089/thy.2008.0021>
18. Fotenos, A.F., Snyder, A.Z., Gitton, L.E., Morris, J.C. and Buckner, R.L., Normative estimates of cross-sectional and longitudinal brain volume decline in aging and AD. Neurology, 64(6), p.1032 (2005). <https://doi.org/10.1212/01.WNL.0000154530.72969.11>
19. Golan, R., Jacob, C. and Denzinger, J., International Joint Conference on Neural Networks (IJCNN), p. 243-(2016).
20. Milletari, F., Ahmadi, S.A., Kroll, C., Plate, A., Rozanski, V., Maiostre, J., Levin, J., Dietrich, O., Ertl-Wagner, B., Bötzel, K. and Navab, N., Computer Vision and Image Understanding, 164, p.92 (2017). <https://doi.org/10.1016/j.cviu.2017.04.002>
21. Perez, L. and Wang, J., The effectiveness of data augmentation in image classification using deep learning. arXiv preprint arXiv:1712.04621.
22. Shie, C.K., Chuang, C.H., Chou, C.N., Wu, M.H. and Chang, E.Y., Transfer representation learning for medical image analysis. 37th annual international conference of the IEEE Engineering in Medicine and Biology Society (EMBC), p.711 (2015). <https://doi.org/10.1109/EMBC.2015.7318461>
23. Garcia-Garcia, A., Orts-Escolano, S., Oprea, S., Villena-Martinez, V., Martinez-Gonzalez, P. and Garcia-Rodriguez, J., Applied Soft Computing, 70, p. 41(2018). <https://doi.org/10.1016/j.asoc.2018.05.018>
24. Baratloo, A., Hosseini, M., Negida, A. and El Ashal, G., p.48 (2015).
25. Lalkhen, A.G. and McCluskey, A., Continuing education in anaesthesia critical care & pain, 8(6), p.221(2008). <https://doi.org/10.1093/bjaceaccp/mkn041>
26. Van Stralen, K.J., Stel, V.S., Reitsma, J.B., Dekker, F.W., Zoccali, C. and Jager, K.J., Kidney international, 75(12), p.1257 (2009). <https://doi.org/10.1038/ki.2009.92>
27. Csurka, G., Larlus, D., Perronnin, F. and Meylan, F., Bmvc, 27, p. 10 (2013).
28. Wong, H.B. and Lim, G.H., Proceedings of Singapore healthcare, 20(4), p.316 (2011). <https://doi.org/10.1177/201010581102000411>
29. Xu, Y., Wang, Y., Yuan, J., Cheng, Q., Wang, X. and Carson, P.L., Ultrasonics, 91, p.1 (2019). <https://doi.org/10.1016/j.ultras.2018.07.006>
30. Badea, M.S., Felea, I.I., Florea, L.M. and Vertan, C., arXiv preprint arXiv:1605.09612 (2016).
31. Kaur, J. and Jindal, A., International Journal of Computer Applications, 50(23), p.1 (2012). <https://doi.org/10.5120/7959-0924>
32. Poudel, P., Illanes, A., Sheet, D. and Friebe, M., Journal of healthcare engineering, (2018). <https://doi.org/10.1155/2018/8087624>
33. Shenoy, N.R. and Jatti, A., Indonesian Journal of Electrical Engineering and Computer Science, 21(3), p.1424 (2021). <https://doi.org/10.11591/ijeecs.v21.i3.pp1424-1434>
34. Garg, H. and Jindal, A., Fourth International Conference on Computing, Communications and Networking Technologies (ICCNT), pp.1 (2013).
35. Frannita, E.L., Nugroho, H.A., Nugroho, A. and Ardiyanto, I., 2nd International Conference on Imaging, Signal Processing and Communication (ICISPC), p. 79(2018).
36. Ying, X., Yu, Z., Yu, R., Li, X., Yu, M., Zhao, M. and Liu, K., International Conference on Neural Information Processing, p.373 (2018). https://doi.org/10.1007/978-3-030-04224-0_32
37. Kumbhakarna, V. M., Kulkarni, S. B., & Dhawale, A. D. (2020). NLP Algorithms Endowed f or Automatic Extraction of Information from Unstructured Free Text Reports of Radiology Monarchy. In International Journal of Innovative Technology and Exploring Engineering (Vol. 9, Issue 12, pp. 338–343). <https://doi.org/10.35940/ijitee.I8009.1091220>
38. Akila, Mrs. P. G., Batri, K., Sasi, G., & Ambika, R. (2019). Denoising of MRI Brain Images using Adaptive Clahe Filtering Method. In International Journal of Engineering and Advanced Technology (Vol. 9, Issue 1s, pp. 91–95). <https://doi.org/10.35940/ijeat.a1018.1091s19>
39. Mounir, M., Redouane, E. B., Reda, M. M., Saad, E. M., & Abderaouf, E. H. (2019). Assessment of the Radiation Dose during 16 Slices CT Examinations. In International Journal of Recent Technology and Engineering (IRTE) (Vol. 8, Issue 4, pp. 4652–4657). <https://doi.org/10.35940/ijrte.d8388.118419>

AUTHOR PROFILE



Jatinder Kumar, Educational Qualification

- Master of Philosophy (Computer Science and Engineering) (2012-13)
- Master of Business Administration (2003-06) from PU, Chandigarh
- Master of computer Application (1994-97) from PU, Chandigarh.
- Bachelor of Science (1991-94) from M.A.M College, Jammu.

Working Experience

- Worked as a Software Engineer in COLTS CONTEC Pvt. Ltd. (Delhi) for One Year.
- Worked as a Computer Science Lecturer in National Institute of Science and Technology JAMMU (Approved by AICTE and Affiliated to Jammu University Limited, Chandigarh for two Years.
- Working in IT Department of PGIMER, Chandigarh since 31-10-2001.
- Area of Interest, Artificial Intelligence (AI), Machine Learning (ML) and Deep Learning (DL) special.

Disclaimer/Publisher's Note: The statements, opinions and data contained in all publications are solely those of the individual author(s) and contributor(s) and not of the Blue Eyes Intelligence Engineering and Sciences Publication (BEIESP)/ journal and/or the editor(s). The Blue Eyes Intelligence Engineering and Sciences Publication (BEIESP) and/or the editor(s) disclaim responsibility for any injury to people or property resulting from any ideas, methods, instructions or products referred to in the content.